



Electrodeposited Co-Pi Catalyst on α -Fe₂O₃ Photoanode for Water-Splitting Applications

M. Toghraei*, H. Siadati

Material Science and Engineering Department, K. N. Toosi University of Technology, Tehran, Iran

PAPER INFO

Paper history:

Received 13 July 2018

Received in revised form 28 October 2018

Accepted 05 December 2018

Keywords:

Solar Water Splitting

Photoanode

Hematite

Co-Pi

Electrodeposition

ABSTRACT

Optoelectronic properties of hematite (α -Fe₂O₃) as a photoanode and the required over-potential in photo-assisted water splitting has been improved by presence of Co-Pi on its surface. In order to increase the lifetime of the photogenerated holes and lower the applied bias, cobalt-phosphate (Co-Pi) on nanostructured α -Fe₂O₃ by electrodeposition was deposited. The nanostructure morphology of the α -Fe₂O₃ was confirmed by XRD and SEM. After depositing four different thicknesses of Co-Pi on α -Fe₂O₃, their photo-electrochemical (PEC) property was determined using linear sweep voltammetry (LSV) and chronoamperometry. The SEM and EDX results showed a complete coverage of Co-Pi on α -Fe₂O₃ and that the Co:P ratio was approximately 1:1.9 for the best produced catalyst. The highest performance of about 200 mV decrease in the onset potential was achieved for the 30-minutes electrodeposited sample. The Co-Pi/ α -Fe₂O₃ catalyst showed an enhancement of 100% of photocurrent compared to the bare α -Fe₂O₃.

doi: 10.5829/ije.2018.31.12c.13

1. INTRODUCTION

The splitting of water by sunlight using a semiconductor has been a subject of interest for almost half a century [1]. Substantial studies have been done on synthetic water oxidation by electro-catalysts that can operate in low over-potentials [2] but frequently required expensive metals or severe pH conditions. As an inexpensive semiconductor, hematite (α -Fe₂O₃) has many desirable properties as a photoanode in a water-splitting photo-electrochemical cell (PEC). It is an n-type semiconductor with a band gap of 2.1 eV, allowing its use in a significantly visible portion of the solar spectrum. It also has a valence band position with a sufficient over-potential for oxidizing water to oxygen [3-6]. Therefore, with chemical stability in aqueous conditions, hematite continues to attract attention as a model photoanode for PEC water oxidation [7]. On the other hand, it suffers from a low rate in the oxygen evolution reaction (OER) during the photo-electrochemical water splitting, i.e. photogenerated

holes accumulate at the surface of the electrode, and a significant charge recombination occurs before the charge transfer across the α -Fe₂O₃/electrolyte interface. This is due to a poor charge mobility (10^{-2} to 10^{-1} cm² s⁻¹ V⁻¹), short diffusion length (2–20 nm), and slow charge-transfer kinetic (10^{-3} to 1 s), causing the solar-to-hydrogen efficiencies to fall due to the rapid electron-hole recombination [7]. Hence, a large over-potential must be applied to achieve significant water-splitting photocurrents [8]. Several studies have shown that this requirement for electrochemical bias can be reduced by using cobalt-phosphate (Co-Pi) [2, 9], with some focusing on improving the Co-Pi/ α -Fe₂O₃ interface [2, 4, 10]. On the one hand, a major drawback of front-side illumination is that absorption losses increase with the thickness of the Co-Pi [7, 11]. On the other hand, transient absorption measurements of Co-Pi/ α -Fe₂O₃ composite catalysts indicate that the photo-generated holes with extended lifetimes apparently accumulate within the α -Fe₂O₃. This leads to the suggestion that Co-Pi does not directly participate in the water-oxidation catalysis but plays an indirect role by inducing additional α -Fe₂O₃ band bending that reduces the electron-hole recombination [7, 9, 10]. Therefore, the

*Corresponding Author Email: masood_764@yahoo.com (M. Toghraei)

aim of this research was to optimize the Co-Pi layer. This layer was electrodeposited on nano-crystalline α -Fe₂O₃ substrates, prepared by the deposition of FeOOH on conductive FTO glass substrates. The photo-electrochemical properties of the Co-Pi/ α -Fe₂O₃ catalysts and the reduction in the required overpotential for water splitting were investigated.

2. MATERIALS METHOD

2.1. α -Fe₂O₃ Electrodes The iron oxide film was electrochemically grown on fluorine doped tin oxide (FTO) glass (FTO-8 Ω Solaronix, Switzerland) in an aqueous solution (10 mM FeCl₃ + 10 mM KF + 0.1 M KCl) (99% Merck) + 1 M H₂O₂ (30%). Anodic deposition was performed at -0.47 to 0.93V (vs Ag/AgCl) with cyclic voltammetry (Autolab PGSTAT30, 50 cycles with a scan rate of 0.1 V/s). The preparation was similar to the procedure mentioned by Schrebler et al. [12]. A common three-electrode electrochemical cell configuration was used, comprising FTO, Pt wire, and Ag/AgCl as working, counter, and reference electrodes, respectively. The electrodeposition was carried out at 50 °C. Before electrodeposition, the FTO glasses were washed with acetone in an ultrasonic bath for 10 minutes. All samples were thoroughly rinsed after their deposition with deionized water and dried with a gentle stream of nitrogen gas. The thin iron oxide film samples were annealed in air for 30 minutes at 650 °C in an atmospheric furnace, to be used as α -Fe₂O₃ electrodes and substrates for Co-Pi electrodeposition.

2.2. Electrodeposition of Co-Pi Layers Co-Pi layers were electrodeposited on α -Fe₂O₃ electrodes under the conditions stipulated earlier [13]. In order to obtain a reasonable assessment of the effect of deposition time on the Co-Pi thickness, and thus the photo-electrochemical behavior of the Co-Pi/ α -Fe₂O₃ catalysts, parameters like bath temperature (room temperature), pressure (1 atm), and pH (7) were kept constant with process time being the only variable parameter. As working electrodes, the α -Fe₂O₃ samples were immersed in an aqueous solution containing 0.5 mM Co (NO₃)₂ and 0.1 M NaH₂PO₄ buffer with pH 7. The saturated Ag/AgCl and Pt wire were used as reference and counter electrodes, respectively. Potentiostatically electrodeposition of Co-Pi layers were carried out at 1.1V (vs. Ag/AgCl) for 5, 15, 30 and 50 minutes (Autolab PGSTAT30). ED5 through ED50 refers to these four samples. At the end of the deposition process, each Co-Pi/ α -Fe₂O₃ samples was rinsed and placed in containers filled with distilled water.

2.3. Characterization The photoelectrochemical experiments were carried out under simulated AM 1.5G

(100 mW cm⁻²) illumination provided by a solar simulator (300 W Xe with optical filter, solar light) in 1 M NaOH (pH = 13.6) solution. Current-voltage measurements were carried out using an Autolab potentiostat in a three-electrode configuration. Co-Pi/ α -Fe₂O₃, Ag/AgCl and platinum wire were used as working, reference, and counter electrodes, respectively. A stainless steel clasp was used to for attaching the top of the FTO, while the lower part was immersed in the electrolyte. All samples were illuminated from the backside (FTO side) of the Co-Pi/ α -Fe₂O₃ catalyst at room temperature and atmospheric pressure.

In order to study the purity and crystallinity of the α -Fe₂O₃, before and after the annealing process, X-ray diffraction (XRD) spectra were acquired using a Philips PW3710 diffractometer (Cu K α = 1.5418 Å). Phase determination was carried out by comparing the results with the corresponding peaks of the JCPDS cards. SEM images were taken using a field emission scanning electron microscope (TESCAN VEGA III) operated at 15 kV. All films were coated with Au, using a thermal evaporator before imaging to diminish charging problems. The chemical analysis of samples was obtained using energy dispersive X-ray spectroscopy (EDX).

3. RESULTS AND DISCUSSION

3.1. Characterization of Structure The XRD peak pattern of the FeOOH deposited on FTO is shown in Figure 1(a). Except the vertical-dashed lines that correspond to the FTO substrate, the other peaks are related to the β -FeOOH phase (JCPDS No. 34-1266) showing its structure, which normally occurs when metal oxides are formed at relatively low temperatures [14]. Figure 1(b) illustrates the corresponding peaks for the annealed sample, confirming that transformation to α -Fe₂O₃ took place as expected (JCPDS No. 86-0550). All samples showed polycrystalline diffraction patterns and the broad peaks indicated the nano-crystallinity of the α -Fe₂O₃ films. Indeed, the oxyhydroxide compounds of Fe(III) transformed into the α -Fe₂O₃ phase upon annealing [12]. The crystalline size of hematite using the Scherrer equation was determined about 56 nm, that was consistent with other reports [15, 16]. The surface morphology of the α -Fe₂O₃ films were evaluated using SEM.

The EDX results for ED30 and ED50 samples are shown in Figure 2. The peaks at 2.05 and 7.1 keV correspond to the presence of phosphorus and cobalt, respectively. The ratio of cobalt to phosphorus (Co:P) in ED30 sample is 1:1.9, which is considerably more than that in ED50 sample (Co:P = 1:0.5), indicating that the growth of Co and P is not simply based on a special molecular formula but is more like an amorphous

structure in which more than one phosphate atom may be contained in each cobalt atom [17]. The presence of phosphate is necessary for the evolution of electrolyte interface promoting oxygen but the precise magnitude of that is not very vital [18-20]. It is important to note that an exact Co:P ratio is not necessary for demonstrating catalytic activity, though the addition of more phosphate assists proton-coupled electron transfer for O₂ evolution [17, 21].

Figure 3 shows the grown α -Fe₂O₃ film on FTO at two different magnifications. It is evident that the hematite film throughout the surface comprises tiny interconnected spheres of around 200 nm diameter. This size is slightly larger than the size determined by the Scherrer equation, but close enough for the SEM resolution.

Figure 4 illustrates the SEM images of the α -Fe₂O₃ surface after electrodeposition of Co:Pi in four different time durations. No evidence of Co-Pi layer was seen on the α -Fe₂O₃ substrate after 5-minute electrodeposition (Figure 4(a)). Increasing the deposition time up to 15 minutes (ED₁₅), showed some scattered Co-Pi particles on the α -Fe₂O₃ surface [Figure 4(b)]. As the electrodeposition time increased to 30 minutes (ED₃₀), on the α -Fe₂O₃ substrate [Figure 4(c)].

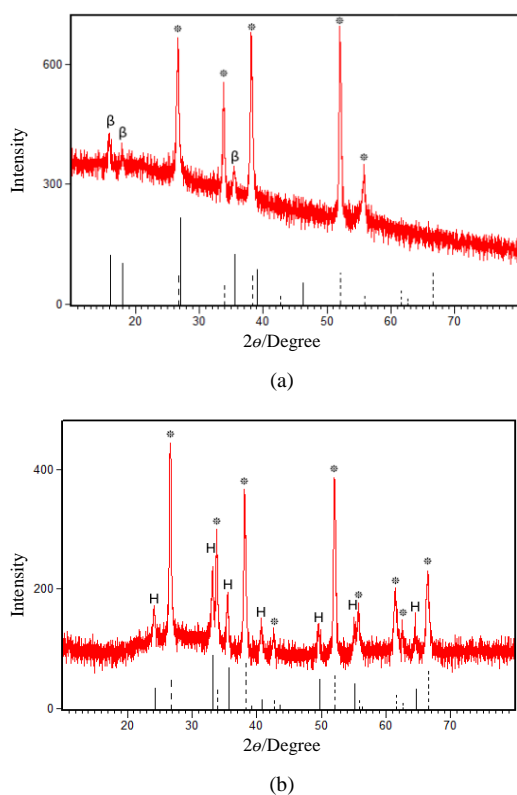


Figure 1. XRD of (a) the as-deposited FeOOH on FTO substrate (the substrate's peaks are indicated with *; the vertical dashed lines) and (b) the emerged α -Fe₂O₃ after annealing (the α -Fe₂O₃ peaks are shown with H)

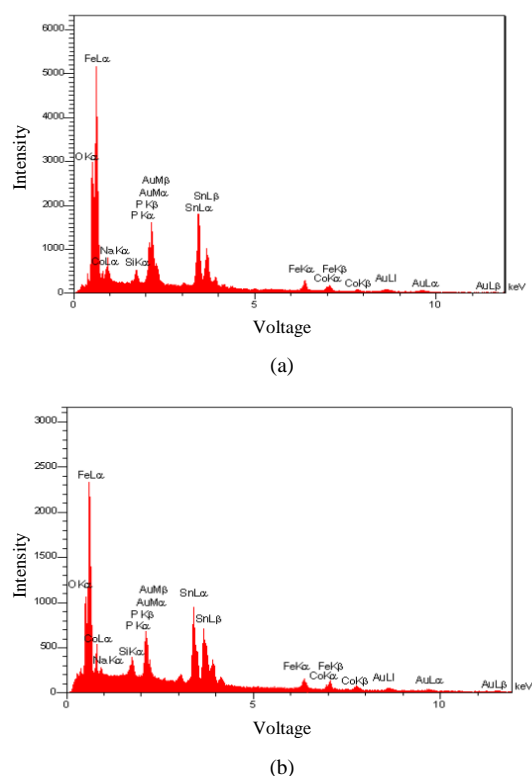


Figure 2. EDX analysis for the samples (a) ED₃₀ and (b) ED₅₀

However, the ED₃₀ sample contained many cracks that seem to have been due to shrinkage. As shown in Figure 4(d), increasing the deposition time to 50 minutes (ED₅₀) brought about a relatively uniform and crack-free layer that covered the α -Fe₂O₃ substrate surface entirely.

3. 2. Photo-Electrochemical Measurements A comparison between current-voltage (*I-E*) characteristics of α -Fe₂O₃ and Co-Pi/ α -Fe₂O₃ samples is shown in Figure 5 by linear sweep voltammetry (LSV). The uppercase A–D and the lowercase a–d represent the dark current and photocurrent vs voltage, respectively.

In the absence of illumination at potentials greater than 0.6 V, the dark current density increases continuously (curve A), indicating the oxidation of water on the surface of α -Fe₂O₃, which is due to an increase in the concentration of free holes in the valence band as the Fermi level is pulled down to a more positive potential approaching the valence band in the region near the surface [22]. At such potentials (≥ 0.6 V), larger increases in the current density occur for the Co-Pi/ α -Fe₂O₃ catalysts corresponding to curves B, C, D, and E. This dark current density enhancement should be the result of water oxidation ($E^0 = 0.23$ V at pH = 13.6) due to the presence of Co-Pi catalyst and not the Co (II) oxidation to Co (III) ($E^0 = 0.82$ V), considering that the more positive potential is required for the later reaction [23].

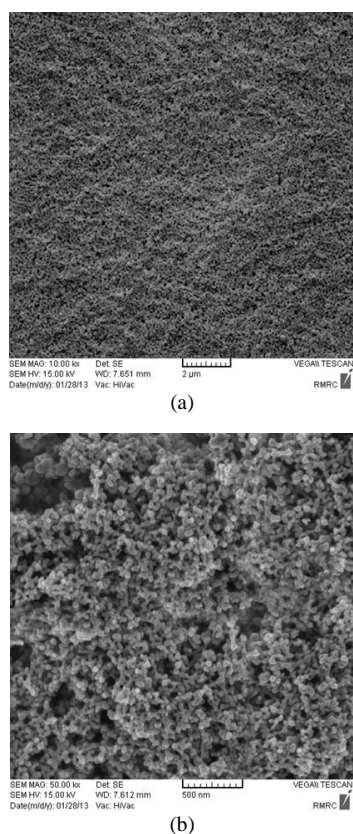


Figure 3. SEM images of α -Fe₂O₃ films

Therefore, the Co-Pi/ α -Fe₂O₃ catalysts require only a small amount of over-potential (~ 0.3 V) for water oxidation; it is about a 0.1 V improvement compared to the bare α -Fe₂O₃ (curve A).

For the illuminated samples, however, the steady-state cathodic shift was observed in the Co-Pi/ α -Fe₂O₃ catalysts compared to the bare α -Fe₂O₃ photoanode. As can be seen in Figure 5 (curves a, b, c, d, and e), a positive photocurrent is observed upon illumination for the electrodes as expected for all n-type photoanodes. Curve “a” reveals that the photocurrent onset potential is at around -0.15 V, because once the applied bias is greater than the flat-band potential, the band bending drives photogenerated holes to the surface for reaction [8]. This potential is much more positive than the flat band of α -Fe₂O₃ (about -0.7 V) [24]. The difference could be due to slow oxidation kinetics (catalysis) and/or to a recombination in the space-charge region. In the curves “b”, “c”, “d”, and “e”, the onset potential is around -0.2 to -0.3 V, similar to the results reported previously for electrodeposited Co-Pi on α -Fe₂O₃ photoanodes [2]. In the illuminated samples, the photocurrent rises rapidly as the potential increases, followed by a potential duration (0.2–0.4) of mild upward rise, and, finally, to exponential convergence. As mentioned, the addition of Co-Pi catalyst to α -Fe₂O₃ has a major effect on the photo-electrochemical

behavior of the bare α -Fe₂O₃. Therefore, in the Co-Pi/ α -Fe₂O₃ electrodes, the required over-potential reduced by about 200 mV. The onset potentials for ED₅, ED₁₅, ED₃₀, and ED₅₀ photoanodes are -0.21 , -0.22 , -0.35 , and -0.29 V, respectively. It is clear that the higher the electrodeposition time of the Co-Pi layers, the further will the curves shift to ever more negative potentials. In other words, the addition of Co-Pi catalyst considerably increased the photocurrent compared to that for the bare α -Fe₂O₃ photoanode. The photocurrent density of the bare α -Fe₂O₃ photoanode from 0.4 mA/cm² increased to 0.7 , 0.69 , 0.8 , and 0.71 mA/cm² for ED₅, ED₁₅, ED₃₀, and ED₅₀ photoanodes, respectively. For the ED₅ and ED₁₅ photoanodes, the small amounts of Co-Pi were not sufficient to cause retardation of electron/hole recombination, which is useful for the water-splitting process. The highest photocurrent was observed in the ED₃₀ sample, perhaps the best coverage in this study since the amount of Co-Pi layer on the hematite electrode causes the reduction of the probability of electron and hole recombination in the structure [17]. The photocurrent of ED₃₀ at 0.23 V vs Ag/AgCl increased 100% with respect to the bare α -Fe₂O₃. Indeed, as observed in Figure 5, at 0.23 V, the current increased by over 100% from around 0.39 mA/cm² to 0.8 mA/cm².

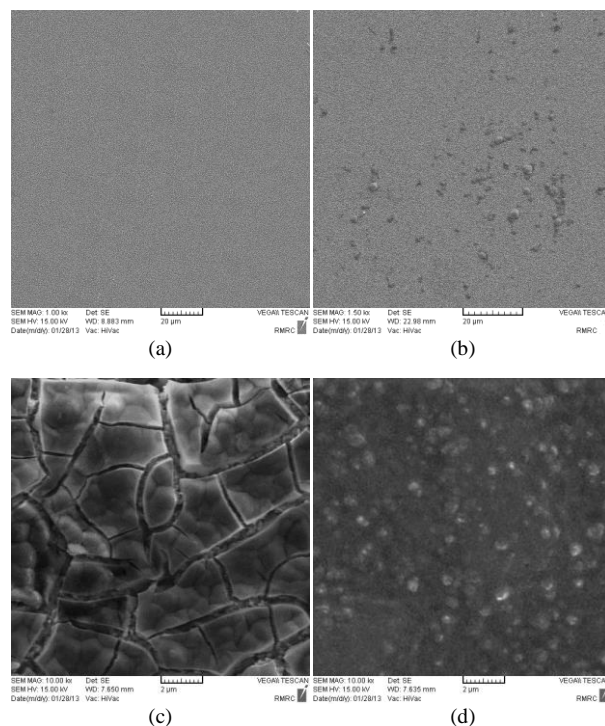


Figure 4. SEM images from the surface of α -Fe₂O₃ after electrodeposition at various time spans: (a) 5 minutes, no Co-Pi layer formed; (b) 15 minutes, scattered Co-Pi catalyst particles; (c) 30 minutes, Co-Pi particles agglomerated and formed a homogenous layer containing cracks; and (d) 50 minutes, a thick and crack free Co-Pi layer

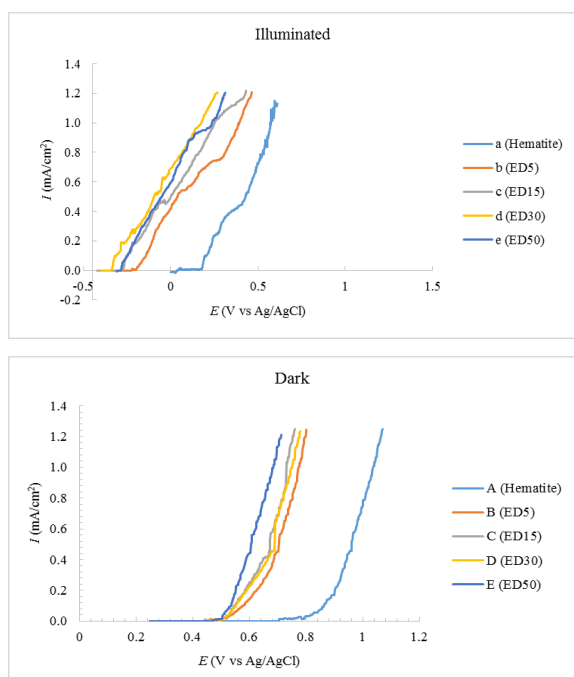


Figure 5. Linear sweep voltammogram of α -Fe₂O₃ (curves a and A) and Co-Pi/ α -Fe₂O₃ samples (b to e and B to E)

A comparison of the EDX and SEM morphologies for ED₃₀ and ED₅₀, suggests that the higher phosphate content, and particularly the presence of cracks on ED₃₀, may have caused the best results in this catalyst. This may be particularly true, specially due to the presence of the cracks, considering the claim that Co-Pi does not directly participate in the water-oxidation catalysis but plays an indirect role by inducing additional α -Fe₂O₃ band bending that reduces the electron-hole recombination [7, 9, 10]. In other words, the cracks on the surface of ED₃₀ may have turned out to be particularly useful. A possible explanation for the role of Co-Pi layer for hampering electron hole recombination could be corresponded to the depletion of electrons in the Fe₂O₃ conduction band, that results in the increase of band bending in the α -Fe₂O₃, leading to the separation of electrons and holes within the α -Fe₂O₃ film and reducing the density of electrons in the vicinity of Co-Pi/ α -Fe₂O₃ interface [25].

Current-Time curves at 0.23 V vs Ag/AgCl for α -Fe₂O₃ and Co-Pi/ α -Fe₂O₃ photoanodes are shown in Figure 6. The photocurrent in the α -Fe₂O₃ sample reached a maximum of 0.62 mA/cm² upon illumination, but rapidly dropped to a minimum and remained constant. As described previously, within the first seconds of irradiation, at low potentials, the Co-Pi/ α -Fe₂O₃ photoanode exhibited a large initial peak current due to the oxidation of the catalyst itself [18, 25].

At higher potentials, however, the observed current should be due to the recombination of the photogenerated charge carriers, indicating the migration

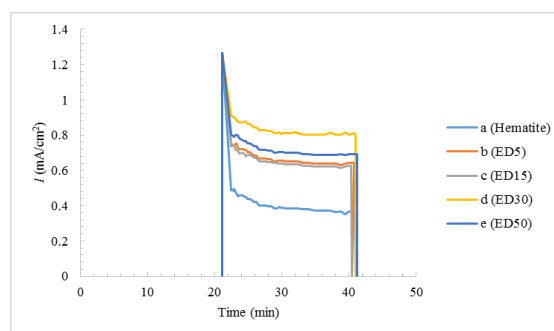


Figure 6. Current-Time curves at 0.23 V vs Ag/AgCl for α -Fe₂O₃ and Co-Pi/ α -Fe₂O₃ catalysts

of holes to the semiconductor/electrolyte interface upon illumination of the photoanode [25]. Therefore, while the initial photocurrent was achieved by an exposure to light, the photocurrent decayed in time, indicating the holes reached the semiconductor surface and recombined with electrons from the conduction band rather than capturing electrons from the electrolyte [26]. Therefore, at a constant potential, the initial currents of the α -Fe₂O₃ and the Co-Pi/ α -Fe₂O₃ are similar, but their final currents differ and the decay of the Co-Pi/ α -Fe₂O₃ electrode is much smaller. This difference in photocurrent decay also indicates the effectiveness of Co-Pi in reducing the recombination of the electron/hole pairs [19]. It is important to note that the steady-state photocurrents at 0.23 V in the four samples—ED₅, ED₁₅, ED₃₀, and ED₅₀—respectively climbed 1.75, 1.7, 2, and 1.8 times higher than that of the bare α -Fe₂O₃ electrode. These results are compatible with those obtained from the linear sweep voltammetry examination and reaffirm that the generated photocurrents are not transient, i.e. they remain constant in time. Evidently, the ED₃₀ sample generated the maximum photocurrent.

4. CONCLUSIONS

Cobalt-phosphate (Co-Pi) layers were prepared at different deposition times on α -Fe₂O₃ by electrodeposition in order to investigate their photoelectrocatalytic performance in sunlight-assisted water splitting. Our research highlighted the importance of the Co-Pi thickness/presence in the modification of α -Fe₂O₃ photoanodes. It could be concluded that Co-Pi increases the lifetime of photogenerated holes in α -Fe₂O₃ and hampers electron-hole recombination, doubling the increase in photocurrent compared to the bare α -Fe₂O₃ photoelectrode. Therefore, the synthesized catalyst is considered as an excellent candidate for solar water-splitting applications, but efforts to extend this strategy for neutral pH waters will be very important for practical water-splitting applications.

5. REFERENCES

1. Fujishima, A., and Honda, K., "Electrochemical Photolysis of Water at a Semiconductor Electrode", *Nature*, Vol. 238, No. 5358, (1972), 37–38.
2. Zhong, D.K., and Gamelin, D.R., "Photoelectrochemical Water Oxidation by Cobalt Catalyst (Co-Pi)/ α -Fe₂O₃ Composite Photoanodes: Oxygen Evolution and Resolution of a Kinetic Bottleneck", *Journal of the American Chemical Society*, Vol. 132, No. 12, (2010), 4202–4207.
3. Shinar, R., and Kennedy, J.H., "Photoactivity of doped α -Fe₂O₃ electrodes", *Solar Energy Materials*, Vol. 6, No. 3, (1982), 323–335.
4. Zhong, D., Cornuz, M., Sivula, K., Grätzel, M., and Gamelin, D.R., "Photo-assisted electrodeposition of cobalt-phosphate (Co-Pi) catalyst on hematite photoanodes for solar water oxidation", *Energy & Environmental Science*, Vol. 4, No. 5, (2011), 1759–1764.
5. Kay, A., Cesar, I., and Grätzel, M., "New benchmark for water photooxidation by nanostructured α -Fe₂O₃ films", *Journal of the American Chemical Society*, Vol. 128, No. 49, (2006), 15714–15721.
6. McDonald, K.J., and Choi, K.-S., "Photodeposition of Co-Based Oxygen Evolution Catalysts on α -Fe₂O₃ Photoanodes", *Chemistry of Materials*, Vol. 23, No. 7, (2011), 1686–1693.
7. Carroll, G.M., Zhong, D.K., and Gamelin, D.R., "Mechanistic insights into solar water oxidation by cobalt-phosphate-modified α -Fe₂O₃ photoanodes", *Energy & Environmental Science*, Vol. 8, No. 2, (2015), 577–584.
8. Van de Krol, R., and Grätzel, M., *Photoelectrochemical Hydrogen Production*, Electronic Materials: Science & Technology; Vol. 102, Springer, (2012).
9. Barroso, M., Cowan, A.J., Pendlebury, S.R., Grätzel, M., Klug, D.R., and Durrant, J.R., "The Role of Cobalt Phosphate in Enhancing the Photocatalytic Activity of α -Fe₂O₃ toward Water Oxidation", *Journal of the American Chemical Society*, Vol. 133, No. 38, (2011), 14868–14871.
10. Barroso, M., Mesa, C.A., Pendlebury, S.R., Cowan, A.J., Hisatomi, T., Sivula, K., Grätzel, M., Klug, D.R., and Durrant, J.R., "Dynamics of photogenerated holes in surface modified α -Fe₂O₃ photoanodes for solar water splitting", *Proceedings of the National Academy of Sciences of the United States of America*, Vol. 109, No. 39, (2012), 15640–15645.
11. Lin, F., and Boettcher, S.W., "Adaptive semiconductor/electrocatalyst junctions in water-splitting photoanodes", *Nature Materials*, Vol. 13, No. 1, (2014), 81–86.
12. Schrebler, R., Bello, K., Vera, F., Cury, P., Muñoz, E., del Río, R., Meier, H.G., Córdova, R., and Dalchiele, E.A., "An electrochemical deposition route for obtaining α -Fe₂O₃ thin films", *Electrochemical and solid-state letters*, Vol. 9, No. 7, (2006), C110–C113.
13. Kanan, M.W., and Nocera, D.G., "In Situ Formation of an Oxygen-Evolving Catalyst in Neutral Water Containing Phosphate and Co²⁺", *Science*, Vol. 321, No. 5892, (2008), 1072–1075.
14. Chirita M, Grozescu I, Taubert L, Radulescu H, Princz E, Stefanovits-Bányai É, Caramalau C, Bulgariu L, Macoveanu M, Muntean, C., "Fe₂O₃-nanoparticles, physical properties and their photochemical and photoelectrochemical applications", *Chemical Bulletin of "POLITEHNICA" University of Timisoara*, Vol. 54, No. 68, (2009), 1–8.
15. Enache, C.S., Liang, Y.Q., and Van de Krol, R., "Characterization of structured α -Fe₂O₃ photoanodes prepared via electrodeposition and thermal oxidation of iron", *Thin Solid Films*, Vol. 520, No. 3, (2011), 1034–1040.
16. Bak, A., Choi, W., and Park, H., "Enhancing the photoelectrochemical performance of hematite (α -Fe₂O₃) electrodes by cadmium incorporation", *Applied Catalysis B: Environmental*, Vol. 110, (2011), 207–215.
17. Shi, X., Zhang, K., and Park, J.H., "Understanding the positive effects of (Co-Pi) co-catalyst modification in inverse-opal structured α -Fe₂O₃-based photoelectrochemical cells", *International Journal of Hydrogen Energy*, Vol. 38, No. 29, (2013), 12725–12732.
18. Surendranath, Y., Kanan, M.W., and Nocera, D.G., "Mechanistic Studies of the Oxygen Evolution Reaction by a Cobalt-Phosphate Catalyst at Neutral pH", *Journal of the American Chemical Society*, Vol. 132, No. 46, (2010), 16501–16509.
19. Lutterman, D.A., Surendranath, Y., and Nocera, D.G., "A Self-Healing Oxygen-Evolving Catalyst", *Journal of the American Chemical Society*, Vol. 131, No. 11, (2009), 3838–3839.
20. Surendranath, Y., Dincă, M., and Nocera, D.G., "Electrolyte-Dependent Electrosynthesis and Activity of Cobalt-Based Water Oxidation Catalysts", *Journal of the American Chemical Society*, Vol. 131, No. 7, (2009), 2615–2620.
21. Steinmiller, E.M.P., and Choi, K.-S., "Photochemical deposition of cobalt-based oxygen evolving catalyst on a semiconductor photoanode for solar oxygen production.", *Proceedings of the National Academy of Sciences of the United States of America*, Vol. 106, No. 49, (2009), 20633–20636.
22. Liang, Y., Enache, C.S., and Van de Krol, R., "Photoelectrochemical Characterization of Sprayed α -Fe₂O₃ Thin Films: Influence of Si Doping and SnO₂ Interfacial Layer", *International Journal of Photoenergy*, Vol. 2008, (2008), 1–7.
23. Smith, R.D.L., Prévot, M.S., Fagan, R.D., Zhang, Z., Sedach, P.A., Siu, M.K.J., Trudel, S., and Berlinguette, C.P., "Photochemical route for accessing amorphous metal oxide materials for water oxidation catalysis", *Science*, Vol. 340, No. 6128, (2013), 60–63.
24. Hahn, N.T., Ye, H., Flaherty, D.W., Bard, A.J., and Mullins, C.B., "Reactive Ballistic Deposition of α -Fe₂O₃ Thin Films for Photoelectrochemical Water Oxidation", *ACS Nano*, Vol. 4, No. 4, (2010), 1977–1986.
25. Kanan, M.W., Surendranath, Y., and Nocera, D.G., "Cobalt-phosphate oxygen-evolving compound", *Chemical Society Reviews*, Vol. 38, No. 1, (2009), 109–114.
26. Bak, T., Nowotny, J., Rekas, M., and Sorrell, C.C., "Photoelectrochemical hydrogen generation from water using solar energy. Materials-related aspects", *International Journal of Hydrogen Energy*, Vol. 27, No. 10, (2002), 991–1022.

Electrodeposited Co-Pi Catalyst on α -Fe₂O₃ Photoanode for Water-Splitting Applications

M. Toghraei, H. Siadati

Material Science and Engineering Department, K. N. Toosi University of Technology, Tehran, Iran

PAPER INFO

چکیده

Paper history:

Received 13 July 2018

Received in revised form 28 October 2018

Accepted 05 December 2018

Keywords:

Solar Water Splitting

Photoanode

Hematite

Co-Pi

Electrodeposition

حضور کبالت-فسفات بر روی سطح هماتیت (α -Fe₂O₃) سبب بهبود خواص اپتوالکترونیک آن به عنوان فوتوآند و کاهش پتانسیل اضافه لازم برای فرایند شکافت آب به کمک تابش نور شده است. در این پژوهش، کبالت-فسفات بر روی نانوساختار α -Fe₂O₃ به طور الکتروکتریکی رسوب داده شد تا زمان حضور حفرات تولیدشده در اثر تابش نور را افزایش داده و بنابراین، بایاس اعمالی را کاهش دهد. مورفولوژی نانوساختار α -Fe₂O₃ بوسیله XRD و SEM تایید شد. پس از رسوب چهار ضخامت مختلف از Co-Pi بر روی α -Fe₂O₃، خواص فوتوالکتروشیمیایی آن‌ها بوسیله ولتامتری روبشی خطی (LSV) و کرومآمپرومتری اندازه‌گیری شد. نتایج SEM و EDX پوشش کامل Co-Pi را بر روی α -Fe₂O₃ با نسبت 1 به 1/9 برای بهترین کاتالیست تولیدی نشان داد. بهترین عملکرد کاهش حدود 200 میلی‌ولت را در پتانسیل شروع جریان آندی برای نمونه با زمان پوشش‌دهی 30 دقیقه نشان داد. کاتالیست Co-Pi/ α -Fe₂O₃ نسبت به نمونه بدون پوشش α -Fe₂O₃ بهبود 100 درصدی را در فوتوجریان تولیدی از خود نشان داد.

doi: 10.5829/ije.2018.31.12c.13